한국동력기계공학회지 제1권 제1호 pp. 124~143 1997년 12월

◉ 연 구 논 문

Dynamics Modeling of Plate Treated with Active Constrained Layer Damping

C. H. Park* and W. C. Kim**

능동 구속층 감쇠 처리된 판의 동적 모델링

박 철 휴* · 김 원 철**

Key Words : Active Constrained Layer Damping(능동구속층 감쇠), Plate(판), Dynamic Modeling(동적 모델링), Finite Element Model(유한요소모델)

요 약

본 논문은 능동 구속층 감쇠(active constrained layer damping) 처리된 판의 동적 모델링과 정식화를 제시한다. 판의 운동방정식은 Hamilton정리를 이용하여 전개된 판, piezoelectric film 및 점탄성층의 운동방정식을 조합하므로서 유도된다. 이 운동방정식은 외부인가전압의 영향하에서 적층판의 해석적 모델을 제공할 뿐만이 아니라, 판 구조내에서 진동에너지를 감소시킬 수 있는 전단층의 효과에 대한 변위관계식을 나타낸다. 그리고 운동방정식에 대응하는 경계조건도 유도되었다. 또한 판과 능동구속층감쇠계의 동특성을 설명하기위한 유한요소모델이 유도되었다. 이 모델의 타당성을 실온조건에서 실험적으로 입증하였다. 개발된 이론 및 실험적인 결과들은 판과 능동구속층 감쇠계가 구조진동의 감쇠를 위한 매우 유효한 수단으로 사용될 수 있음을 나타내었다.

NOMENCLATURE

A	Surface area of plate
d	Distance ($d=h_3+h_2/2+h_4/2$) in Fig. 1
$[d_{ij}]$	Piezoelectric strain/charge constant matrix
D_s	Electric displacement
$[D_{ij}]$	Flexural rigidity matrix
$\{E\}$	Applied field strength matrix
E_1, E_2, E_3, E_4	Moduli of elasticity of base plate, piezo-sensor, viscoelastic core and piezo-actuator, respectively
$\{F_{pk}\}$	Control force vector
G_3	Complex shear modulus of the viscoelastic core
h_1, h_2, h_3, h_4	Thicknesses of base plate, piezo-sensor, viscoelastic core and

* Engineering Science and Mechanics, Virginia Polytechnic Institute and State University
** The Institute of Marine Industry, Gyeongsang National University

	piezo-actuator, respectively
H	Total thickness of ACLD/plate system ($H=h_1+h_2+h_3+h_4$)
I_i	Moment of inertia of i-th layer
$[K_i]$	Stiffness matrix of the i-th element
k_d, k_p	Derivative and proportional control gain
L	Length of plate
$[M_i]$	Mass matrix of the i-th element
$\{M_{pk}\}$	Control moment vector
$[N_i]$	Interpolation matrices
$q_i(x,y,t)$	Lateral body force of i-th layer
$[Q_{ij}]$	Plane stress-reduced stiffnesses matrix with respect to lamina axes
$\{T\}$	Stress matrix
u_0	In-plane longitudinal displacements of the neutral plane along x-axis
u_1, u_2, u_4	Longitudinal deflection of neutral axes of base plate, piezo-sensor and piezo-actuator along x-axis
v_0	In-plane longitudinal displacements of the neutral plane along y-axis
v_1, v_2, v_4	Longitudinal deflection of neutral axes of base plate, piezo-sensor and piezo-actuator along y-axis
V_3	Applied electric field
w	Transverse deflection of ACLD for plates
x y z	Fixed reference frame

Greek Symbols

γ_{xz}, γ_{yz}	Distortion angles of the shear layer
η	Loss factor
ν	Poisson's ratio
Θ_x, Θ_y	Slope in the x, y directions
ρ_1, ρ_2, ρ_3, ρ_4	Mass density of base plate, piezo-sensor, viscoelastic core, and piezo-actuator
$\{\Delta_i\}$	Nodal deflection
ω^*	Complex angular frequency
$\Delta(x,y)$	Generalized location function of the piezo-sensor

1. INTRODUCTION

The theoretical studies of the smart structures have drawn much attention due to their effectiveness of damping out structural vibrations in order to avoid structural damage due to fatigue, reducing the life cycle. This paper presents a new class of Actively-controlled Constrained Layer Damping(ACLD) treatment that can be an effective means for damping out the vibrations of large flexible structures. The proposed ACLD consists of a viscoelastic damping layer that is sandwiched between two piezoelectric layers. The three-layer composite ACLD when bonded to a vibrating surface acts as a smart constrained layer damping treatment with built-in sensing and actuation capabilities [Fig.1].

The piezoelectric sensing layer monitors the structural oscillation due to the direct piezoelectric effect and the actuator suppresses the oscillation via the converse piezoelectric effect. This dual effect, which does not exist in conventional constrained damping layers, significantly contributes to the damping effectiveness of the smart ACLD. In this manner, the smart ACLD consists of a conventional passive constrained layer damping which is augmented with the described dual effect to actively control the strain of the constrained layer, in response to the structural vibrations.

Recently, considerable emphasis has been

placed on controlling the vibration of plates using various passive and active control strategies. Important among these strategies is the passive Electro-Mechanical Surface Damping (EMSD)[1] approach and the Intelligent Constrained Layer (ICL)[2] damping treatment. In both strategies, the vibrating plate is treated with a viscoelastic damping layer which is constrained by a piezo-electric film. The piezo-film is utilized to generate additional damping through the use of shunting circuits tuned to the dominant resonant frequencies of the vibrating plate as in the EMSD approach, or through controlling the shear deformation of the viscoelastic treatment as in the ICL approach.

In the present paper, the focus is placed on comprehensive modeling and control of multi-modes of vibration of plates using Newtonian and variational formulations of plates with ACLD treatments.

The mathematical model is introduced to describe the interaction between the vibrating structure, piezo-electric sensor/actuator and viscoelastic damping. The model is based on the well-known shear damping model[3,4] which have been extensively used to analyze the dynamics of passive constrained layer damping. The shear damping model is integrated with the models describing the behavior of the distributed piezo-electric sensor and distributed piezo-electric actuator[5] to generate ACLD model. The equation of motion of plate/ACLD system is derived to couple the lateral vibration of the base plate, the in-plane vibration of the base plate, and the in-plane vibrations of piezo-electric sheets. The theoretical modeling involves the development of a finite element model to describe the dynamics and control of flexible plates treated fully with the acld treatment. Also the theoretical models are validated experimentally at various operating conditions to demonstrate the merits of the plate/ACLD as an effective means for suppressing the vibration of the flat plates.

2. CONSTITUTIVE EQUATION OF PLATE/ACLD SYSTEM

The ACLD for plates consists of a base plate layer (1), a sensor layer (2) and a constraining actuator layer (4), sandwiching a viscoelastic core layer (3) shown in Fig. 1 which is a schematic drawing of the ACLD treatment for plates. The plate has length L, thickness h_1, elastic modulus E_1 and density ρ_1. The sensor sheet has thickness h_2, Young's modulus E_2 and mass density ρ_2. The piezo-electric actuator has thickness h_4, Young's modulus E_4 and piezo-electric constant d_{31}. The viscoelastic layer has the thickness h_3, mass density ρ_3, complex shear modulus G_3 and Young's modulus E_3, $G_3 = G'(1+i\eta_3)$ and $E_3 = E'(1+i\eta_3)$, where the superscript' indicates the elastic modulus and η_3 is the loss factor which is frequency and temperature dependent. In the sequel, the subscript p denotes the base plate, s the sensor, v the viscoelastic, and a the actuator.

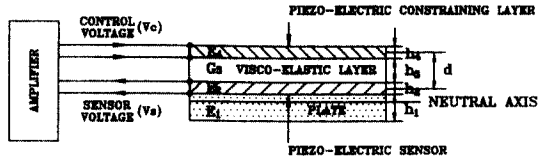

Fig. 1 A schematic drawing of four layer plate/ACLD system

The assumptions made in the foregoing analysis are:

1) A plane transverse to the middle plane before bending, remains plane and perpendicular to the middle plane after bending.
2) The transverse displacement w at a section does not vary along thickness.
3) The piezo-sensor/actuator layers and the base plate are assumed to be elastic and isotropic.
4) The viscoelastic layer is assumed to be linearly viscoelastic and characterized by a complex modulus G_3. The extensional effect in the shear layer is ignored for the case of a soft core.
5) Perfect bonding between meeting surfaces is assumed.

These assumptions make physical sense and are generally made in the analysis of constrained layer damping treatments.

Kirchhoff's classical plate hypothesis is applied to the longitudinal displacements u_i and v_i and the strains of the base plate, sensor, and actuator layer as follows:

$$u_p = u_1 - z\frac{\partial w}{\partial x}, \qquad v_p = v_1 - z\frac{\partial w}{\partial y}. \tag{1}$$

$$u_s = u_2 - z\frac{\partial w}{\partial x}, \qquad v_c = v_2 - z\frac{\partial w}{\partial y}. \tag{2}$$

$$u_a = u_4 - z\frac{\partial w}{\partial x}, \qquad v_a = v_4 - z\frac{\partial w}{\partial y}, \tag{3}$$

where z is the distance from the mid-surface of each layer.

The longitudinal displacement components u_v and v_v of the shear layer can be determined for the geometry of ACLD treatment, shown in Fig. 2, as follows:

$$u_v = \left(\frac{u_4 + u_2}{2}\right) + \left(\frac{\partial w}{\partial x}\right)\left(\frac{h_2 - h_4}{4}\right), \tag{4}$$

$$v_v = \left(\frac{v_4 + v_2}{2}\right) + \left(\frac{\partial w}{\partial y}\right)\left(\frac{h_2 - h_4}{4}\right). \tag{5}$$

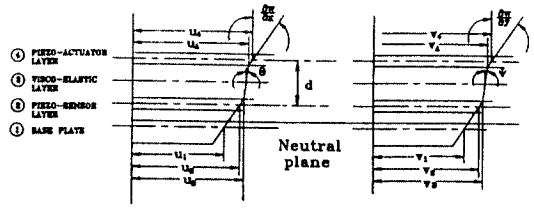

Fig. 2 Theoretical parameters of plate/ACLD System

The strains of each layer can be expressed in a convenient form, where the membrane strains and bending strains are separated as follows:

$$[\varepsilon_1]_p = \frac{\partial u_1}{\partial x} - z\left(\frac{\partial^2 w}{\partial x^2}\right), \quad [\varepsilon_2]_p = \frac{\partial v_1}{\partial y} - z\left(\frac{\partial^2 w}{\partial y^2}\right),$$
$$[\varepsilon_6]_p = \frac{\partial u_1}{\partial y} + \frac{\partial v_1}{\partial x} - 2z\left(\frac{\partial^2 w}{\partial x \partial y}\right), \tag{6}$$

$$[\varepsilon_1]_s = \frac{\partial u_2}{\partial x} - z\left(\frac{\partial^2 w}{\partial x^2}\right), \quad [\varepsilon_2]_s = \frac{\partial v_2}{\partial y} - z\left(\frac{\partial^2 w}{\partial y^2}\right), \quad [\varepsilon_6]_s =$$
$$\frac{\partial u_2}{\partial y} + \frac{\partial v_2}{\partial x} - 2z\left(\frac{\partial^2 w}{\partial x \partial y}\right), \quad [\varepsilon_1]_a = \frac{\partial u_4}{\partial x} - z\left(\frac{\partial^2 w}{\partial x^2}\right) -$$
$$d_{31}E_3\Lambda(x,y), \quad [\varepsilon_2]_a = \frac{\partial v_4}{\partial y} - z\left(\frac{\partial^2 w}{\partial y^2}\right) - d_{32}E_3\Lambda(x,y) \tag{7}$$

and

$$[\varepsilon_6]_a = \frac{\partial u_4}{\partial y} + \frac{\partial v_4}{\partial x} - 2z\left(\frac{\partial^2 w}{\partial x \partial y}\right), \tag{8}$$

where $\Lambda(x,y)$ is a distribution shape function of the sensor [$\Lambda(x,y)$=1 for uniform sensor] and the constants d_{31} and d_{32} are termed the piezoelectric strain constants and are defined to be the ratio of developed free strain to the applied voltage (units of m/v).

The shear strains γ_{xz} and γ_{yz} of the viscoelastic core can be written as:

$$[\gamma_{xx}]_v = \left(\frac{d}{h_3}\right)\left[\left(\frac{u_4-u_2}{d}\right)-\left(\frac{\partial w}{\partial x}\right)\right], \quad [\gamma_{yx}]_v = \left(\frac{d}{h_3}\right)\left[\left(\frac{v_4-v_2}{d}\right)-\left(\frac{\partial w}{\partial y}\right)\right] \tag{9}$$

where $d=(h_3+h_2/2+h_1/2)$ with h_2, h_3 and h_1 denoting the thicknesses of the sensor, the viscoelastic core and actuator layer, respectively.

The corresponding stress components of the base plate are given by

$$[\sigma_1]_p = \frac{E_1}{1-\nu_1^2}\left[\left(\frac{\partial u_1}{\partial x}+\nu_1\frac{\partial v_1}{\partial y}\right)-z\left(\frac{\partial^2 w}{\partial x^2}+\nu_1\frac{\partial^2 w}{\partial y^2}\right)\right], \tag{10}$$

$$[\sigma_2]_p = \frac{E_1}{1-\nu_1^2}\left[\left(\frac{\partial v_1}{\partial y}+\nu_1\frac{\partial u_1}{\partial x}\right)-z\left(\frac{\partial^2 w}{\partial y^2}+\nu_1\frac{\partial^2 w}{\partial x^2}\right)\right], \tag{11}$$

$$[\sigma_6]_p = \frac{E_1}{2(1+\nu_1)}\left[\left(\frac{\partial u_1}{\partial y}+\frac{\partial v_1}{\partial x}\right)-2z\left(\frac{\partial^2 w}{\partial x \partial y}\right)\right]. \tag{12}$$

For the sensor layer are

$$[\sigma_1]_s = \frac{E_2}{1-\nu_2^2}\left[\left(\frac{\partial u_2}{\partial x}+\nu_2\frac{\partial v_2}{\partial y}\right)-z\left(\frac{\partial^2 w}{\partial x^2}+\nu_2\frac{\partial^2 w}{\partial y^2}\right)\right], \tag{13}$$

$$[\sigma_2]_s = \frac{E_2}{1-\nu_2^2}\left[\left(\frac{\partial v_2}{\partial y}+\nu_2\frac{\partial u_2}{\partial x}\right)-z\left(\frac{\partial^2 w}{\partial y^2}+\nu_2\frac{\partial^2 w}{\partial x^2}\right)\right], \tag{14}$$

$$[\sigma_6]_s = \frac{E_2}{2(1+\nu_2)}\left[\left(\frac{\partial u_2}{\partial y}+\frac{\partial v_2}{\partial x}\right)-2z\left(\frac{\partial^2 w}{\partial x \partial y}\right)\right]. \tag{15}$$

For the actuator layer are

$$[\sigma_1]_a = \frac{E_4}{1-\nu_4^2}\left[\left(\frac{\partial u_4}{\partial x}+\nu_4\frac{\partial v_4}{\partial y}\right)-z\left(\frac{\partial^2 w}{\partial x^2}+\nu_4\frac{\partial^2 w}{\partial y^2}\right)\right] - \left(\frac{E_4}{1-\nu_4^2}\right)\left(\frac{V_3\Lambda(x,y)}{h_4}\right)(d_{31}+\nu_4 d_{32}), \tag{16}$$

$$[\sigma_2]_a = \frac{E_4}{1-\nu_4^2}\left[\left(\frac{\partial v_4}{\partial y}+\nu_4\frac{\partial u_4}{\partial x}\right)-z\left(\frac{\partial^2 w}{\partial y^2}+\nu_4\frac{\partial^2 w}{\partial x^2}\right)\right] - \left(\frac{E_4}{1-\nu_4^2}\right)\left(\frac{V_3\Lambda(x,y)}{h_4}\right)(d_{32}+\nu_4 d_{31}), \tag{17}$$

$$[\sigma_6]_a = \frac{E_4}{2(1+\nu_4)}\left[\left(\frac{\partial u_4}{\partial y}+\frac{\partial v_4}{\partial x}\right)-2z\left(\frac{\partial^2 w}{\partial x \partial y}\right)\right], \tag{18}$$

where V_3 is the voltage across the thickness direction of the piezo lamina. Also, E_i and ν_i denote Young's modulus and Poisson's ratio of layer i where i: 1,2 and 4.

The shear stresses in the viscoelastic layer are given by

$$[\tau_{xx}]_v = G_3[\gamma_{xx}]_v, \quad [\tau_{yx}]_v = G_3[\gamma_{yx}]_v. \tag{19}$$

Hence, The stress resultants can be found by integrating the equations (10) through (18) in the normal direction. Also equations (10) through (18) were multiplied by z and integrated across the thickness of each lamina, then the moment resultants can be obtained as follows:

$$\begin{bmatrix} N_1 \\ N_2 \\ N_6 \end{bmatrix}_i = \int_{-h_i/2}^{h_i/2}\begin{bmatrix} \sigma_1 \\ \sigma_2 \\ \sigma_6 \end{bmatrix}_i dz, \quad \begin{bmatrix} M_1 \\ M_2 \\ M_6 \end{bmatrix}_i = \int_{-h_i/2}^{h_i/2}\begin{bmatrix} \sigma_1 \\ \sigma_2 \\ \sigma_6 \end{bmatrix}_i z\, dz \quad i = p, s \text{ and } a \tag{20}$$

where N_1 and N_2 are the normal stress resultants, N_6 is the shear stress resultant, M_1 and M_2 are the normal moment resultants, M_6 is the twisting moment resultant. Moreover, the shear resultants Q_x and Q_y for viscoelastic shear layer are written as follows:

$$[Q_x]_v = h_3[\tau_{xx}]_v, \quad [Q_y]_v = h_3[\tau_{yx}]_v. \tag{21}$$

3. EQUATIONS OF MOTION USING NEWTONIAN FORMULATION

The equations of motion of plate/ACLD system are derived using Newton's laws in this section. In vector mechanics, a representative volume element of the body is isolated with all its applied and reactive forces, i.e., a free-body diagram [Fig.3] is used, and the governing equations of motion are obtained by summing forces and moments. Thus, the vector mechanics approach is closer to physical intuition.

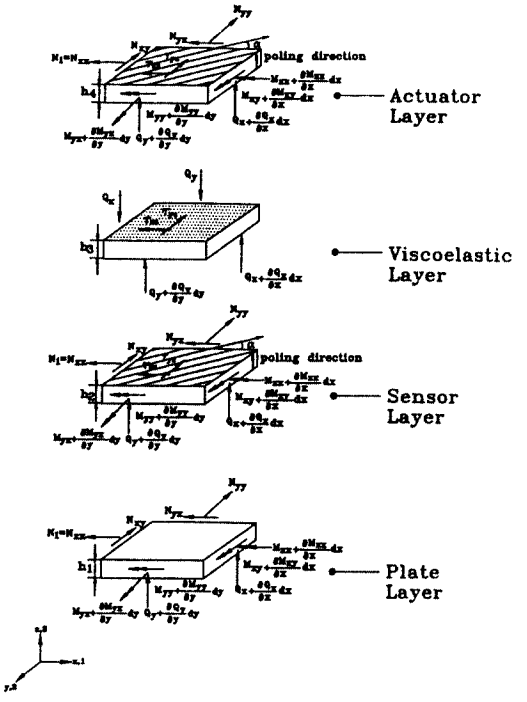

Fig. 3 Free body diagram of the plate/ACLD system

$$\left(\frac{\partial N_1}{\partial x}\right)_p+\left(\frac{\partial N_6}{\partial y}\right)_p=\rho_1 h_1\frac{\partial^2 u_1}{\partial t^2}\,, \tag{22}$$

$$\left(\frac{\partial N_2}{\partial y}\right)_p+\left(\frac{\partial N_6}{\partial x}\right)_p=\rho_1 h_1\frac{\partial^2 v_1}{\partial t^2}\,, \tag{23}$$

$$\left(\frac{\partial^2 M_1}{\partial x^2}\right)_p+2\left(\frac{\partial^2 M_6}{\partial x\partial y}\right)_p+\left(\frac{\partial^2 M_2}{\partial y^2}\right)_p=\rho_1 h_1\frac{\partial^2 w}{\partial t^2}+$$

$$q_p(x,y,t)\,, \tag{24}$$

and

$$\left(\frac{\partial N_1}{\partial x}\right)_{s,a}+\left(\frac{\partial N_6}{\partial y}\right)_{s,a}\pm\left(\tau_{xz}\right)_{s,a}=\rho_{2,4}h_{2,4}\frac{\partial^2 u_{2,4}}{\partial t^2}\,, \tag{25}$$

$$\left(\frac{\partial N_2}{\partial y}\right)_{s,a}+\left(\frac{\partial N_6}{\partial x}\right)_{s,a}\pm\left(\tau_{yz}\right)_{s,a}=\rho_{2,4}h_{2,4}\frac{\partial^2 v_{2,4}}{\partial t^2}\,, \tag{26}$$

$$\left(\frac{\partial^2 M_1}{\partial x^2}\right)_{s,a}+2\left(\frac{\partial^2 M_6}{\partial x\partial y}\right)_{s,a}+\left(\frac{\partial^2 M_2}{\partial y^2}\right)_{s,a}+$$

$$\frac{h_{2,4}}{2}\left(\frac{\partial\tau_{xz}}{\partial x}+\frac{\partial\tau_{yz}}{\partial y}\right)_{s,a}=\rho_{2,4}h_{2,4}\frac{\partial^2 w}{\partial t^2}+q_{s,a}(x,y,t)\,, \tag{27}$$

where i = p, a, s and u_i, v_i are the mid-plane displacements along the x and y directions of a base plate, sensor, and actuator respectively. w is the displacement in the z direction, $q_i(x,y,t)$ is the lateral body forces.

In addition, Newton's second law applied to the lateral direction for viscoelastic shear layer results in

$$h_3\left(\frac{\partial\tau_{xz}}{\partial x}+\frac{\partial\tau_{yz}}{\partial y}\right)+q_v=\rho_3 h_3\frac{\partial^2 w}{\partial t^2} \tag{28}$$

Adding the equations (24), (27), and (28) and substituting the stress and moment resultants from equation (20) into the equations of motion (22) through (27), the differential equations of plate/ACLD system are obtained as follows:

$$\frac{E_1 h_1}{(1-\nu_1^2)}\left[\left(\frac{\partial^2 u_1}{\partial x^2}\right)+\frac{(1+\nu_1)}{2}\left(\frac{\partial^2 v_1}{\partial x \partial y}\right)+\left(\frac{1-\nu_1}{2}\right)\left(\frac{\partial^2 u_1}{\partial y^2}\right)\right]$$

$$=\rho_1 h_1\left(\frac{\partial^2 u_1}{\partial t^2}\right), \tag{29}$$

$$\frac{E_1 h_1}{(1-\nu_1^2)}\left[\left(\frac{\partial^2 v_1}{\partial y^2}\right)+\frac{(1+\nu_1)}{2}\left(\frac{\partial^2 u_1}{\partial x \partial y}\right)+\left(\frac{1-\nu_1}{2}\right)\left(\frac{\partial^2 v_1}{\partial x^2}\right)\right]$$

$$=\rho_1 h_1\left(\frac{\partial^2 v_1}{\partial t^2}\right), \tag{30}$$

and

$$\frac{E_2 h_2}{(1-\nu_2^2)}\left[\left(\frac{\partial^2 u_2}{\partial x^2}\right)+\frac{(1+\nu_2)}{2}\left(\frac{\partial^2 v_2}{\partial x \partial y}\right)+\left(\frac{1-\nu_2}{2}\right)\left(\frac{\partial^2 u_2}{\partial y^2}\right)\right]$$

$$+G_3\left[\frac{u_4-u_2}{h_3}-\frac{d}{h_3}\left(\frac{\partial w}{\partial x}\right)\right]=\rho_2 h_2\left(\frac{\partial^2 u_2}{\partial t^2}\right), \tag{31}$$

$$\frac{E_2 h_2}{(1-\nu_2^2)}\left[\left(\frac{\partial^2 v_2}{\partial y^2}\right)+\frac{(1+\nu_2)}{2}\left(\frac{\partial^2 u_2}{\partial x \partial y}\right)+\left(\frac{1-\nu_2}{2}\right)\left(\frac{\partial^2 v_2}{\partial y^2}\right)\right]$$

$$+G_3\left[\frac{v_4-v_2}{h_3}-\frac{d}{h_3}\left(\frac{\partial w}{\partial y}\right)\right]=\rho_2 h_2\left(\frac{\partial^2 v_2}{\partial t^2}\right), \tag{32}$$

and

$$\frac{E_4 h_4}{(1-\nu_4^2)}\left[\left(\frac{\partial^2 u_4}{\partial x^2}\right)+\frac{(1+\nu_4)}{2}\left(\frac{\partial^2 v_4}{\partial x \partial y}\right)+\left(\frac{1-\nu_4}{2}\right)\left(\frac{\partial^2 u_4}{\partial y^2}\right)\right]$$

$$-G_3\left[\frac{u_4-u_2}{h_3}-\frac{d}{h_3}\left(\frac{\partial w}{\partial x}\right)\right]=\rho_4 h_4\left(\frac{\partial^2 u_4}{\partial t^2}\right)+\frac{\partial \Lambda}{\partial x}(C_{11}d_{31}+$$

$$C_{12}d_{32})+\frac{\partial \Lambda}{\partial y}(C_{61}d_{31}+C_{62}d_{32}), \tag{33}$$

$$\frac{E_4 h_4}{(1-\nu_4^2)}\left[\left(\frac{\partial^2 v_4}{\partial y^2}\right)+\frac{(1+\nu_4)}{2}\left(\frac{\partial^2 u_4}{\partial x \partial y}\right)+\left(\frac{1-\nu_4}{2}\right)\left(\frac{\partial^2 v_4}{\partial y^2}\right)\right]$$

$$-G_3\left[\frac{v_4-v_2}{h_3}-\frac{d}{h_3}\left(\frac{\partial w}{\partial y}\right)\right]=\rho_4 h_4\left(\frac{\partial^2 v_4}{\partial t^2}\right)+\frac{\partial \Lambda}{\partial x}(C_{61}d_{31}+$$

$$C_{62}d_{32})+\frac{\partial \Lambda}{\partial y}(C_{21}d_{31}+C_{22}d_{32}), \tag{34}$$

and

$$\frac{E_1 h_1^3}{12(1-\nu_1^2)}\left[\frac{\partial^4 w}{\partial x^4}+2\frac{\partial^4 w}{\partial x^2 \partial y^2}+\frac{\partial^4 w}{\partial y^4}\right]+\frac{E_2 h_2^3}{12(1-\nu_2^2)}\left[\frac{\partial^4 w}{\partial x^4}+\right.$$

$$\left.2\frac{\partial^4 w}{\partial x^2 \partial y^2}+\frac{\partial^4 w}{\partial y^4}\right]+\frac{E_4 h_4^3}{12(1-\nu_4^2)}\left[\frac{\partial^4 w}{\partial x^4}+2\frac{\partial^4 w}{\partial x^2 \partial y^2}+\frac{\partial^4 w}{\partial y^4}\right]$$

$$-G_3\frac{d}{h_3}\left[\left(\frac{\partial u_4}{\partial x}-\frac{\partial u_2}{\partial x}\right)+\left(\frac{\partial v_4}{\partial y}-\frac{\partial v_2}{\partial y}\right)-d\left(\frac{\partial^2 w}{\partial x^2}+\frac{\partial^2 w}{\partial y^2}\right)\right]$$

$$+\rho h\frac{\partial^2 w}{\partial t^2}=q(x,y,t)-\frac{\partial^2 \Lambda}{\partial x^2}(H_{11}d_{31}+H_{12}d_{32})-2\frac{\partial^2}{\partial x \partial y}$$

$$(H_{61}d_{31}+H_{62}d_{32})-\frac{\partial^2 \Lambda}{\partial y^2}(H_{21}d_{31}+H_{22}d_{32}), \tag{35}$$

where $\rho=\rho_1 h_1+\rho_2 h_2+\rho_3 h_3+\rho_4 h_4$ is the overall mass density and q is total body force of the system. The elements C_{ij} and H_{ij} are defined as follows:

$$C_{ij}=[Q_{ij}]V_3, \qquad H_{ij}=z_a[Q_{ij}]V_3, \tag{36}$$

where $[Q_{ij}]$ are referred to as the plane stress-reduced stiffnesses of the film lamina with respect to the reference axes (x, y, z) which is given by:

$$[Q]=\begin{bmatrix} \cos^2\alpha & \sin^2\alpha & -2\cos\alpha\sin\alpha \\ \sin^2\alpha & \cos^2\alpha & 2\cos\alpha\sin\alpha \\ \cos\alpha\sin\alpha & -\cos\alpha\sin\alpha & \cos^2\alpha-\sin^2\alpha \end{bmatrix}$$

$$\begin{bmatrix} \frac{E_a}{1-\nu_a^2} & \frac{\nu_a E_a}{1-\nu_a^2} & 0 \\ \frac{\nu_a E_a}{1-\nu_a^2} & \frac{E_a}{1-\nu_a^2} & 0 \\ 0 & 0 & \frac{E_a}{2(1+\nu_a)} \end{bmatrix} \tag{37}$$

with defining the skew angle between the actuator piezoelectric axis and the x axis as shown in Fig. 3. Also z_a is the moment arm from neutral surface to the mid-surface of the actuator layer. The above equations govern the dynamic behavior of the

plate/ACLD system under the action of the applied electric field V_3 and the transverse mechanical loading q.

4. EQUATIONS OF MOTION USING VARIATIONAL FORMULATION

The equations of motion of a ACLD for plates using energy principles are developed. The energy principles require the minimization of the total potential energy to derive the equations of motion and associated boundary conditions. To get the differential equations of the ACLD for plates using variational principles, requires the development of the kinetic energy and potential energy.

The strain energy U_t stored over the volume of the ACLD for linear elastic behavior is given by evaluating the following integral:

$$U_t = \frac{1}{2}\iiint_V \sum_{\substack{i=1,2,3\\ j=p,s,a}} \left(\left[\varepsilon_i\right]_j^T\left[\sigma_i\right]_j\right)dV. \tag{38}$$

Substituting equations (6) through (19) into equation (38) and performing the integration over the thickness of each layer, the total strain energy of the plate/ACLD system is obtained as follows:

$$U_t = \frac{E_1 h_1}{2(1-\nu_1^2)}\iint_A\left[\left(\frac{\partial u_1}{\partial x}\right)^2 + 2\nu_1\left(\frac{\partial u_1}{\partial x}\right)\left(\frac{\partial v_1}{\partial y}\right) + \left(\frac{\partial v_1}{\partial y}\right)^2 + \frac{1-\nu_1}{2}\left(\frac{\partial u_1}{\partial y} + \frac{\partial v_1}{\partial x}\right)^2\right]dxdy + \frac{E_1 h_1^3}{24(1-\nu_1^2)}\iint_A\left[\left(\frac{\partial^2 w}{\partial x^2}\right)^2 + 2\nu_1\left(\frac{\partial^2 w}{\partial x^2}\right)\left(\frac{\partial^2 w}{\partial y^2}\right) + \left(\frac{\partial^2 w}{\partial y^2}\right)^2 + 2(1-\nu_1)\left(\frac{\partial^2 w}{\partial x \partial y}\right)^2\right]dxdy$$

$$+ \frac{E_2 h_2}{2(1-\nu_2^2)}\iint_A\left[\left(\frac{\partial u_2}{\partial x}\right)^2 + 2\nu_2\left(\frac{\partial u_2}{\partial x}\right)\left(\frac{\partial v_2}{\partial y}\right) + \left(\frac{\partial v_2}{\partial y}\right)^2 + \frac{1-\nu_2}{2}\left(\frac{\partial u_2}{\partial y} + \frac{\partial v_2}{\partial x}\right)^2\right]dxdy + \frac{E_2 h_2^3}{24(1-\nu_2^2)}\iint_A\left[\left(\frac{\partial^2 w}{\partial x^2}\right)^2 + 2\nu_2\left(\frac{\partial^2 w}{\partial x^2}\right)\left(\frac{\partial^2 w}{\partial y^2}\right) + \left(\frac{\partial^2 w}{\partial y^2}\right)^2 + 2(1-\nu_2)\left(\frac{\partial^2 w}{\partial x \partial y}\right)^2\right]dxdy$$

$$+ \frac{E_4 h_4}{2(1-\nu_4^2)}\iint_A\left[\left(\frac{\partial u_4}{\partial x}\right)^2 + 2\nu_4\left(\frac{\partial u_4}{\partial x}\right)\left(\frac{\partial v_4}{\partial y}\right) + \left(\frac{\partial v_4}{\partial y}\right)^2 + \frac{1-\nu_4}{2}\left(\frac{\partial u_4}{\partial y} + \frac{\partial v_4}{\partial x}\right)^2\right]dxdy + \frac{E_4 h_4^3}{24(1-\nu_4^2)}\iint_A\left[\left(\frac{\partial^2 w}{\partial x^2}\right)^2 + 2\nu_4\left(\frac{\partial^2 w}{\partial x^2}\right)\left(\frac{\partial^2 w}{\partial y^2}\right) + \left(\frac{\partial^2 w}{\partial y^2}\right)^2 + 2(1-\nu_4)\left(\frac{\partial^2 w}{\partial x \partial y}\right)^2\right]dxdy$$

$$+ \iint_A \Lambda(x,y)\left[\bar{C}_{31}\left(\frac{\partial u_4}{\partial x}\right) + \bar{C}_{32}\left(\frac{\partial v_4}{\partial y}\right) + \bar{C}_{36}\left(\frac{\partial u_4}{\partial y} + \frac{\partial v_4}{\partial x}\right)\right]dxdy + \iint_A \Lambda(x,y)\left[\bar{H}_{31}\left(\frac{\partial^2 w}{\partial x^2}\right) + \bar{H}_{32}\left(\frac{\partial^2 w}{\partial y^2}\right) + 2\bar{H}_{36}\left(\frac{\partial^2 w}{\partial x \partial y}\right)\right]dxdy + \frac{1}{2}\iint_A G_3 h_3\left\{\left(\frac{u_4-u_2}{h_3}\right)^2 + \left(\frac{v_4-v_2}{h_3}\right)^2 - 2\frac{d}{h_3}\left[\left(\frac{u_4-u_2}{h_3}\right)\left(\frac{\partial w}{\partial x}\right) + \left(\frac{v_4-v_2}{h_3}\right)\left(\frac{\partial w}{\partial y}\right)\right] + \left[\left(\frac{\partial w}{\partial x}\right)^2 + \left(\frac{\partial w}{\partial y}\right)^2\right]\left(\frac{d}{h_3}\right)^2\right\}dxdy. \tag{39}$$

with $\bar{H}_{ij} = z_e\,\bar{C}_{ij}$ where

$$\bar{C}_{31} = C_{11}d_{31} + C_{12}d_{32} + C_{16}d_{36} = V_3\frac{E_e}{(1-\nu_e^2)}\left[d_{31}\left(m^2 + \nu_e n^2\right) + d_{32}\left(n^2 + \nu_e m^2\right) - d_{36}mn\left(1-\nu_e\right)\right], \tag{40}$$

$$\bar{C}_{32} = C_{21}d_{31} + C_{22}d_{32} + C_{26}d_{36} = V_3\frac{E_e}{(1-\nu_e^2)}\left[d_{31}\left(n^2 + \nu_e m^2\right) + d_{32}\left(m^2 + \nu_e n^2\right) + d_{36}mn\left(1-\nu_e\right)\right], \tag{41}$$

and

$$\bar{C}_{36} = C_{61}d_{31} + C_{62}d_{32} + C_{66}d_{36}$$

$$= V_3 \frac{E_c}{(1+\nu_c)}\left[(d_{31}-d_{32})mn + \frac{1}{2}d_{36}(m^2-n^2)\right], \quad (42)$$

and $m = \cos\alpha$, $n = \sin\alpha$, α is the skew angle.

The kinetic energy T_t of the ACLD for plates element can be calculated from:

$$T_t = \frac{1}{2}\iiint \sum_{j=p,s,a,v} \rho_j\left[\left(\frac{\partial w}{\partial t}\right)^2 + \left(\frac{\partial u_j}{\partial t}\right)^2 + \left(\frac{\partial v_j}{\partial t}\right)^2\right] dxdydz . \quad (43)$$

Substituting equations (1) through (5) into equation (43), then the total kinetic energy is obtained as follows:

$$T_t = \frac{\rho_1 h_1 + \rho_2 h_2 + \rho_3 h_3 + \rho_4 h_4}{2}\iint_A \left(\frac{\partial w}{\partial t}\right)^2 dxdy + \frac{1}{2}\iint_A \left\{\rho_1 h_1\left[\left(\frac{\partial u_1}{\partial t}\right)^2 + \left(\frac{\partial v_1}{\partial t}\right)^2\right] + \rho_2 h_2\left[\left(\frac{\partial u_2}{\partial t}\right)^2 + \left(\frac{\partial v_2}{\partial t}\right)^2\right] + \rho_4 h_4\left[\left(\frac{\partial u_4}{\partial t}\right)^2 + \left(\frac{\partial v_4}{\partial t}\right)^2\right] + \left\{\frac{\rho_1 h_1^3 + \rho_2 h_2^3 + \rho_4 h_4^3}{12}\left[\left(\frac{\partial^2 w}{\partial x \partial t}\right)^2 + \left(\frac{\partial^2 w}{\partial y \partial t}\right)^2\right]\right\} dxdy + \frac{1}{2}\iint_A \rho_3 h_3\left\{\left[\frac{1}{2}\left(\frac{\partial u_4}{\partial t} + \frac{\partial u_2}{\partial t}\right) + \left(\frac{\partial^2 w}{\partial x \partial t}\right)\left(\frac{h_2 - h_4}{4}\right)\right]^2 + \left[\frac{1}{2}\left(\frac{\partial v_4}{\partial t} + \frac{\partial v_2}{\partial t}\right) + \left(\frac{\partial^2 w}{\partial y \partial t}\right)\left(\frac{h_2 - h_4}{4}\right)\right]^2\right\} dxdy + \frac{1}{2}\iint_A \frac{\rho_3 h_3}{12}\left\{\left[\left(\frac{\partial u_4}{\partial t} - \frac{\partial u_2}{\partial t}\right) - \left(\frac{\partial^2 w}{\partial x \partial t}\right)\left(\frac{h_4 + h_2}{2}\right)\right]^2 + \left[\left(\frac{\partial v_4}{\partial t} - \frac{\partial v_2}{\partial t}\right) - \left(\frac{\partial^2 w}{\partial y \partial t}\right)\left(\frac{h_4 + h_2}{2}\right)\right]^2\right\} dxdy . \quad (44)$$

It can be seen that the kinetic energy of the plate/ACLD system is composed of two parts. The first represents the kinetic energy due to in-plane and out-of-plane displacements in the x, y, z directions. The second part involves the two angular velocities of the system about x and y axes times the mass moment inertia for this element.

The work done on the plate/ACLD system by the external loads q is expressed in the following form:

$$V_t = \iint_A q(x,y,t)w\,dxdy . \quad (45)$$

Applying Hamilton's principle to find the equations of motion of the system along with all the natural and geometric boundary conditions gives:

$$\delta H_t = \delta\int_{t_1}^{t_2}(T_t - U_t - V_t)dt = 0, \quad (46)$$

where t_1 and t_2 are the end points in the time domain. The boundary conditions are obtained as follows :

A) Along $x = 0$ and $x = a$:

$$\text{either } u_1 = 0, \text{ or } \frac{E_1 h_1}{(1-\nu_1^2)}\left(\frac{\partial u_1}{\partial x} + \nu_1\frac{\partial v_1}{\partial y}\right) = 0, \quad (47)$$

$$\text{either } v_1 = 0, \text{ or } \frac{E_1 h_1}{2(1+\nu_1)}\left(\frac{\partial v_1}{\partial x} + \frac{\partial u_1}{\partial y}\right) = 0, \quad (48)$$

$$\text{either } u_2 = 0, \text{ or } \frac{E_2 h_2}{(1-\nu_2^2)}\left(\frac{\partial u_2}{\partial x} + \nu_2\frac{\partial v_2}{\partial y}\right) = 0, \quad (49)$$

$$\text{either } v_2 = 0, \text{ or } \frac{E_2 h_2}{2(1+\nu_2)}\left(\frac{\partial v_2}{\partial x} + \frac{\partial u_2}{\partial y}\right) = 0, \quad (50)$$

$$\text{either } u_4 = 0, \text{ or } \frac{E_4 h_4}{(1-\nu_4^2)}\left(\frac{\partial u_4}{\partial x} + \nu_4\frac{\partial v_4}{\partial y}\right) = \Lambda(x,y)\left[C_{11}d_{31} + C_{12}d_{32}\right], \quad (51)$$

either $v_4 = 0$, or $\frac{E_4 h_4}{2(1+\nu_4)}\left(\frac{\partial v_4}{\partial x}+\frac{\partial u_4}{\partial y}\right) = \Lambda(x,y)$

$\left[C_{61}d_{31}+C_{62}d_{32}\right]$, (52)

either $w = 0$, or

$\frac{E_1 h_1^3}{12(1-\nu_1^2)}\left(\frac{\partial^3 w}{\partial x^3}+(2-\nu_1)\frac{\partial^3 w}{\partial x \partial y^2}\right)+\frac{E_2 h_2^3}{12(1-\nu_2^2)}\left(\frac{\partial^3 w}{\partial x^3}+\right.$

$\left.(2-\nu_2)\frac{\partial^3 w}{\partial x \partial y^2}\right)\ \frac{E_4 h_4^3}{12(1-\nu_4^2)}\left(\frac{\partial^3 w}{\partial x^3}+(2-\nu_4)\frac{\partial^3 w}{\partial x \partial y^2}\right)+$

$G_3 d\left[\frac{u_4-u_2}{h_3}-\left(\frac{d}{h_3}\right)\left(\frac{\partial w}{\partial x}\right)\right]+\frac{\partial \Lambda}{\partial x}\left(H_{11}d_{31}+H_{12}d_{32}\right)+$

$2\frac{\partial \Lambda}{\partial y}\left(H_{61}d_{31}+H_{62}d_{32}\right)=0$, (53)

either $\frac{\partial w}{\partial x} = 0$, or

$\frac{E_1 h_1^3}{12(1-\nu_1^2)}\left(\frac{\partial^2 w}{\partial x^2}+\nu_1\frac{\partial^2 w}{\partial y^2}\right)+\frac{E_2 h_2^3}{12(1-\nu_2^2)}\left(\frac{\partial^2 w}{\partial x^2}+\nu_2\frac{\partial^2 w}{\partial y^2}\right)$

$+\frac{E_4 h_4^3}{12(1-\nu_4^2)}\left(\frac{\partial^2 w}{\partial x^2}+\nu_4\frac{\partial^2 w}{\partial y^2}\right)+\left[H_{11}d_{31}\Lambda(x,y)+\right.$

$\left.H_{12}d_{32}\Lambda(x,y)\right]=0$. (54)

B) Along $y = 0$ and $y = b$:

either $u_1 = 0$, or $\frac{E_1 h_1}{2(1+\nu_1)}\left(\frac{\partial u_1}{\partial y}+\frac{\partial v_1}{\partial x}\right)=0$, (55)

either $v_1 = 0$, or $\frac{E_1 h_1}{(1-\nu_1^2)}\left(\frac{\partial v_1}{\partial y}+\nu_1\frac{\partial u_1}{\partial x}\right)=0$, (56)

either $u_2 = 0$, or $\frac{E_2 h_2}{2(1+\nu_2)}\left(\frac{\partial u_2}{\partial y}+\frac{\partial v_2}{\partial x}\right)=0$, (57)

either $v_2 = 0$, or $\frac{E_2 h_2}{(1-\nu_2^2)}\left(\frac{\partial v_2}{\partial y}+\nu_2\frac{\partial u_2}{\partial x}\right)=0$, (58)

either $u_4 = 0$, or $\frac{E_4 h_4}{2(1+\nu_4)}\left(\frac{\partial u_4}{\partial y}+\frac{\partial v_4}{\partial x}\right)=$

$\Lambda(x,y)\left[C_{61}d_{31}+C_{62}d_{32}\right]$, (59)

either $v_4 = 0$, or $\frac{E_4 h_4}{(1-\nu_4^2)}\left(\frac{\partial v_4}{\partial y}+\nu_4\frac{\partial u_4}{\partial x}\right)=\Lambda(x,y)$

$\left[C_{21}d_{31}+C_{22}d_{32}\right]$, (60)

either $w = 0$, or

$\frac{E_1 h_1^3}{12(1-\nu_1^2)}\left(\frac{\partial^3 w}{\partial y^3}+(2-\nu_1)\frac{\partial^3 w}{\partial y \partial x^2}\right)+\frac{E_2 h_2^3}{12(1-\nu_2^2)}\left(\frac{\partial^3 w}{\partial y^3}+\right.$

$\left.(2-\nu_2)\frac{\partial^3 w}{\partial y \partial x^2}\right)\ \frac{E_4 h_4^3}{12(1-\nu_4^2)}\left(\frac{\partial^3 w}{\partial y^3}+(2-\nu_4)\frac{\partial^3 w}{\partial y \partial x^2}\right)+$

$G_3 d\left[\frac{v_4-v_2}{h_3}-\left(\frac{d}{h_3}\right)\left(\frac{\partial w}{\partial y}\right)\right]+\frac{\partial \Lambda}{\partial y}\left(H_{21}d_{31}+H_{22}d_{32}\right)+$

$2\frac{\partial \Lambda}{\partial x}\left(H_{61}d_{31}+H_{62}d_{32}\right)=0$, (61)

either $\frac{\partial w}{\partial x} = 0$, or

$\frac{E_1 h_1^3}{12(1-\nu_1^2)}\left(\frac{\partial^2 w}{\partial y^2}+\nu_1\frac{\partial^2 w}{\partial x^2}\right)+\frac{E_2 h_2^3}{12(1-\nu_2^2)}\left(\frac{\partial^2 w}{\partial y^2}+\nu_2\frac{\partial^2 w}{\partial x^2}\right)$

$+\frac{E_4 h_4^3}{12(1-\nu_4^2)}\left(\frac{\partial^2 w}{\partial y^2}+\nu_4\frac{\partial^2 w}{\partial x^2}\right)+\left[H_{21}d_{31}\Lambda(x,y)+\right.$

$\left.H_{22}d_{32}\Lambda(x,y)\right]=0$. (62)

C) Reaction force of the corner for a free edge

$2\left[\frac{E_1 h_1^3}{12(1+\nu_1)}+\frac{E_2 h_2^3}{12(1+\nu_2)}+\frac{E_3 h_3^3}{12(1+\nu_3)}\right]\frac{\partial^2 w}{\partial x \partial y}+\left(H_{61}d_{31}+\right.$

$\left.H_{62}d_{32}\right)=0$. (63)

These boundary conditions render the solution of the differential equations of the plate/ACLD system unique. Equation (63) shows how the twisting moment generated by the electro-mechanical interaction of the piezoelectric film will affect the natural boundary condition of the plate/ACLD system.

5. FINITE ELEMENT FORMULATION

The plate/ACLD elements considered are two-dimensional elements bounded by four nodal points. Each node has five degrees of freedom to describe the longitudinal displacements u and v, transverse deflection w and the slopes $\partial w/\partial x$ and $\partial w/\partial y$ of the deflection line. These deflections are assumed to be given in the following form of polynomials in the local coordinate variables x and y:

$$u = a_1 + a_2x + a_3y + a_4xy, \quad v = a_5 + a_6x + a_7y + a_8xy, \tag{64}$$

and

$$w = b_1 + b_2x + b_3y + b_4x^2 + b_5xy + b_6y^2 + b_7x^3 + b_8x^2y + b_9xy^2 + b_{10}y^3 + b_{11}x^3y + b_{12}xy^3. \tag{65}$$

The constants $\{a_1, a_2, \ , a_8\}$ and $\{b_1, b_2, \ , b_{12}\}$ are determined in terms of the twenty components of the nodal deflection vector $\{\Delta_i\}$ of the i-th element which is bounded by the nodes. Displacements within an element are interpolated from element nodal degree of freedom, $\{\Delta\} = \{u, v, w, \Theta_x, \Theta_y\}^T$, at any location (x,y) inside the i-th element can be determined from:

$$\{u, v, w, \Theta_x, \Theta_y\}^T = \{[N_1], [N_2], [N_3], [N_4], [N_5]\}^T \{\Delta_i\}, \tag{66}$$

where $[N_1]$, $[N_2]$, $[N_3]$, $[N_4]$ and $[N_5]$ are the spatial interpolating vectors corresponding to u, v, w, and respectively. Using the strain-displacement relationships, the strain vector is obtained as follows:

$$\{\varepsilon\} = [d]\{\Delta\} = [d][N]\{\Delta_i\} = [B]\{\Delta_i\}, \tag{67}$$

where $[d]$ is called a linear differential operator and $[B]$ is the strain-displacement matrix.

By substituting the discretized expression for strain-displacement terms into variational equation, the equations of motion of the ACLD-treated plate element in nodal displacement are derived as the following form:

$$[M_i]\{\ddot{\Delta}_i\} + [K_i]\{\Delta_i\} = \{F_c\} \tag{68}$$

where $[K_i]$ and $[M_i]$ denote the stiffness and mass matrices of the plate/ACLD element which are obtained by the strain energy [mechanical part of equation (39)] and kinetic energy [equation 44)].

$$U_{mech.} = \frac{1}{2}\iiint_v [\varepsilon]^T[\sigma]dv = \frac{1}{2}\{\Delta_i\}^T[K_i]\{\Delta_i\}, \text{ where}$$

$$[K] = \iiint_v [B]^T[E][B]dV \tag{69}$$

$$T_{total} = \frac{1}{2}\iiint_v \rho_i\left[\dot{w}^2 + \dot{u}_i^2 + \dot{v}_i^2\right]dxdydz = \frac{1}{2}\{\Delta_i\}^T[M_i]\{\Delta_i\},$$

$$\text{where } [M] = \iiint_v \rho[N]^T[N]dV, \ i=1, 2, 3, 4. \tag{70}$$

The vector $\{F_c\}$ is the vector of control forces and moments generated by the piezo-constraining layer on the treated plate element. It is expressed as follows:

$$\{F_c\} = \{F_1, F_2, F_3, F_4\}^T, \tag{71}$$

where

$$\{F_i\}=\{F_{pxi}, F_{pyi}, 0, M_{pxi}, M_{pyi}\}^T \quad \text{for } i=1,\ldots,4, \tag{72}$$

where F_{pxi}, F_{pyi}, M_{pxi} and M_{pyi} denote the control forces and moments generated at node i which is obtained by the strain energy [electrical part of equation (39)] as follows:

$$U_{elec.}=\iint_A \Lambda(x,y)\left[\bar{C}_{31}\left(\frac{\partial u_4}{\partial x}\right)+\bar{C}_{32}\left(\frac{\partial v_4}{\partial y}\right)+\bar{C}_{36}\left(\frac{\partial u_4}{\partial y}+\frac{\partial v_4}{\partial x}\right)\right]dxdy+\iint_A \Lambda(x,y)\left[\bar{H}_{31}\left(\frac{\partial^2 w}{\partial x^2}\right)+\bar{H}_{32}\left(\frac{\partial^2 w}{\partial y^2}\right)+2\bar{H}_{36}\left(\frac{\partial^2 w}{\partial x \partial y}\right)\right]dxdy. \tag{73}$$

6. EXPERIMENTAL IMPLEMENTATION

The experimental performance of the fully and partially treated plate/ACLD system is determined for different control gains in this section. The ACLD full treatment which is 25.4 cm long and 12.7 cm wide is mounted in a cantilevered base plate (Alloy 3003 aluminum sheet) to act as a smart constraining layer damping treatment with built-in sensing and actuation capabilities. The viscoelastic layer sheet of DYAD-606 from Soundcoat is sandwiched by two piezoelectric layers from AMP Inc.. In this regard, a plate with full ACLD and half treatments is tested at different control gains while operating at room temperature (25℃). Hence, the effect of proportional and derivative control action on the system performance is presented. The experimental work in this section aims also at demonstrating the merits of the ACLD as an effective means for suppressing the vibration of the flat plates.

Tables 1 and 2 list the main physical and geometrical parameters of the aluminum sheet, DYAD-606 and polymeric films (Model number S028NAO). The performance of viscoelastic material is affected by the temperature and frequency which, in turn, influence the shear modulus and the loss factor.

Table 1 Physical and geometrical properties of the plate, viscoelastic and PVDF layer

Layer	Thickness (m)	Young's Modulus (Pa)	Density (kg/m^3)	Poisson's ratio (v)
ALUMINUM	4.064E-4	7.1E10	2700	0.33
DYAD-606	5.08E-5	*	1105	0.49
PVDF	2.8E-5	2.5E9	1780	0.3

*** Depending on temperature and frequency**

Table 2 The main piezo-electric parameters of the PVDF film(at room temperature

d_{31} (m/V)	d_{32} (m/V)	d_{33} (m/V)	k_{31} (%)	k_{33}
23E-12	3E-12	-33E-12	10	12

The schematic drawings of the full and half treatments for ACLD is shown in the Fig.4. A uniformly distributed piezo-actuator is used to control the first two bending modes of the plate/ACLD system.

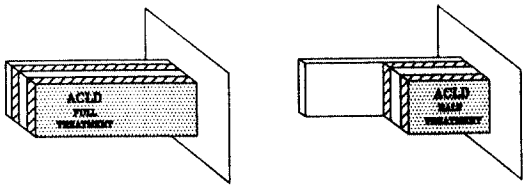

Fig. 4 Schematic drawings for full and half ACLD treatments

Fig. 5 shows a schematic drawing of the experimental setup used in testing the effectiveness of the active constrained layer damping in attenuating the vibration of the test plate as compared with conventional passive constrained layer damping. The internal function generator of the spectrum analyzer (Model CF910, ONO SOKKI) is used to generate a sine-wave sweep linearly from 0 Hz to 35 Hz with a sweep rate 0.025 Hz/sec. This sine wave is used to acoustically excite the plate/ACLD system through a loud speaker powered by power amplifier (Model 6260, Urel Electronic Co.). The tip displacement signal is measured by laser sensor (Model MQ-Aeromat Corp., Providence, NJ.) at the middle-end of the test plate and is fed to the spectrum analyzer (ONO SOKKI Model CF910) to determine its frequency content. The laser sensor has an accuracy of 20 m over a frequency band between 0~1000 Hz. The magnitude ratio (dB) and the phase shift (deg) of the system response are automatically displayed and stored in the analyzer. Thus, the transfer function between the input and output can be obtained. Fig. 5 also shows that another spectrum analyzer (Model CF-350, ONO SOKKI) is independently used to obtain the transfer function between the piezo-actuator and piezo-sensor. The signal from the piezoelectric sensor is amplified using a charge amplifier (Model AM-5 from Wilcoxon Research, Rockville, MD). An analog circuit is used to generate a proportional and derivative control law. An analog filter (Model 432, Waveteck Co.) is then used to filter out the high frequency content to avoid observation spillover. The resulting control action is sent via an analog power amplifier (Model PA7C, Wilcoxon Research) to the piezoelectric actuator layer and the spectrum analyzer (Model CF-350, ONO SOKKI) to determine the frequency content and the amplitude of vibration.

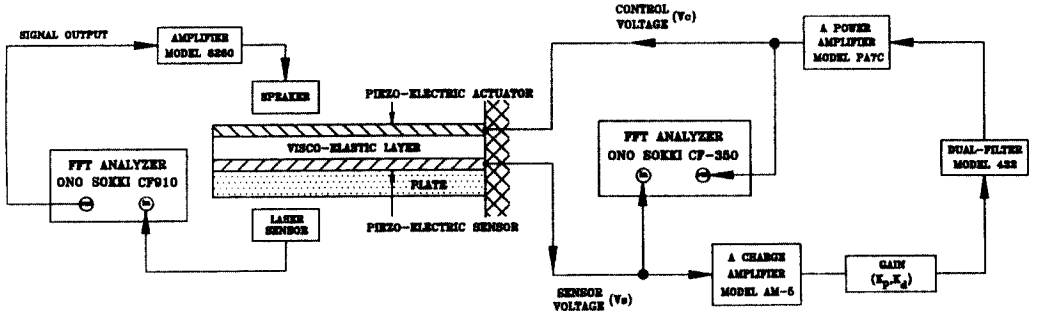

Fig. 5 Schematic drawing of the experiment setup

7. EXPERIMENTAL RESULTS BETWEEN HALF AND FULL TREATMENT

The experimental results cover two ranges of frequencies. The first range (1~15 Hz) includes the first bending mode and the second second (20~40 Hz) covers the second bending resonant frequency. Comparisons are shown between the amplitudes of vibration when the ACLD is unactivated (i.e., it acts as a conventional Passive Constrained Layer Damping - PCLD) and when it is activated using three different proportional control gains at a fixed temperature. In addition, tests on partial ACLD treatment are also performed.

A comparison between the natural frequencies, loss factors and attenuations for the half and full treatment plate/ACLD system at temperature 25℃ is shown. The amplitude values listed are computed from the transverse deflection w of the free middle end of the plate due to a sine-wave sweep from 0 Hz to 35 Hz. The effects of using the half ACLD treatment are shown in Tables 3 through 6 and Fig. 6 a) through Fig. 7 a) when a proportional and/or derivative

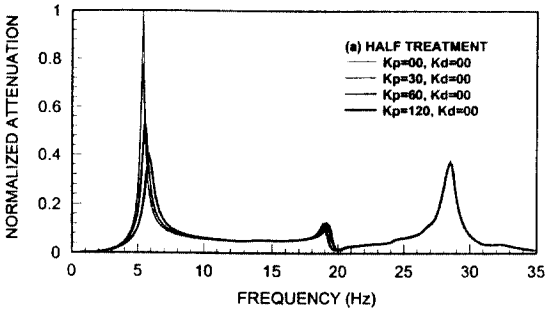

(a) half treatment

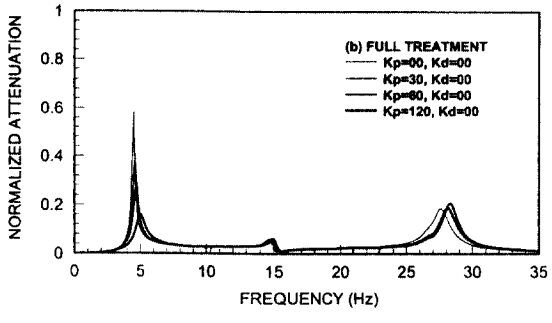

(b) full treatment

Fig. 6 The frequency response of normalized attenuation of vibration amplitude for ACLD controlled by k_p [only] at temperature 25℃

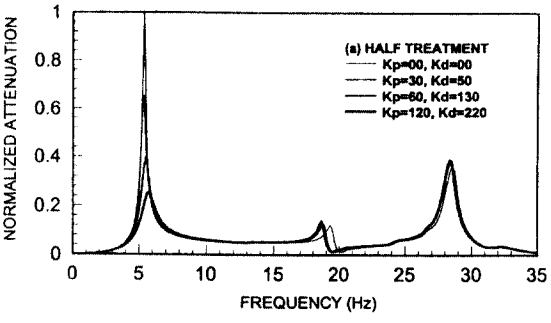

(a) half treatment

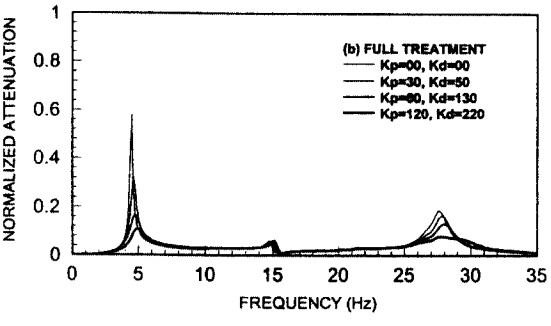

(b) full treatment

Fig. 7 The frequency response of normalized attenuation of vibration amplitude for ACLD controlled by k_p and k_d at temperature 25℃

Table 3 The natural frequencies, loss factors and attenuations of the first bending mode for half ACLD treatment at temperature 25℃

T:25°C	First bending mode			
k_p(only)	Frequency	Loss factor	Amplitude	Attenuation
k_p=00	5.37	0.046	405.76	
k_p=30	5.37	0.055	314.46	22.55%
k_p=60	5.62	0.072	215.01	46.86%
k_p=120	5.87	0.130	160.23	60.52%

Table 4 The natural frequencies, loss factors and attenuations of the second bending mode for half ACLD treatment at temperature 25℃

T:25°C	Second bending mode			
k_p(only)	Frequency	Loss factor	Amplitude	Attenuation
k_p=00	28.55	0.032	148.64	
k_p=30	28.47	0.031	152.74	-2.0%
k_p=60	28.50	0.031	152.84	-2.8%
k_p=120	28.52	0.032	151.60	-1.9%

Table 5 The natural frequencies, loss factors and attenuations of the first bending mode for half ACLD treatment at temperature 25℃

T:25°C	First bending mode			
k_p, k_d	Frequency	Loss factor	Amplitude	Attenuation
k_p=00, k_d=00	5.37	0.046	405.76	
k_p=30, k_d=50	5.37	0.061	266.53	34.32%
k_p=60, k_d=130	5.50	0.109	159.40	60.71%
k_p=120, k_d=220	5.75	0.171	102.83	74.66%

Table 6 The natural frequencies, loss factors and attenuations of the second bending mode for half ACLD treatment at temperature 25℃

T:25°C	Second bending mode			
k_p, k_d	Frequency	Loss factor	Amplitude	Attenuation
k_p=00, k_d=00	28.55	0.032	148.64	
k_p=30, k_d=50	28.42	0.030	153.64	-3.0%
k_p=60, k_d=130	28.45	0.029	154.50	-3.9%
k_p=120, k_d=220	28.43	0.030	159.37	-7.2%

control law is employed. Fig. 6 a) and Fig. 7 a) indicate that the amplitudes of the first bending modes for half ACLD treatment are considerably attenuated as compared to those of the PCLD (k_p=0, k_d=0) for all the proportional and derivative control gains. However, increasing the control gains produces insignificant attenuations of the second bending mode due to the treatment geometry as shown in the Fig. 4. Tables 7 and 8 list the natural frequencies, loss factors and attenuations for the full ACLD treatment when controlled by only proportional control actions at room temperature 25℃. Fig. 6 b) shows that the vibration amplitudes of the first bending are effectively reduced when the proportional control gains are increased. For example, the attenuations of 29.4%, 52.3% and 72.4% are obtained when k_p is set at 30, 60 and 120 respectively.

It is evident that increasing k_p (only) did not result in improving the vibration attenuation characteristics of the second bending mode. The performance, however, is improved by augmenting the proportional controller with a derivative component as shown in Fig. 7 b). According to Table 7, when the optimal gains (k_p=120 and k_d=220) are set at temperature of 25℃, the attenuation of amplitude of first bending mode is 81.4% shown in Table 9. Such attenuation is due to the activation of the ACLD treatment which results in increasing the damping ratio about four times that of the unactivated ACLD (i.e., the PCLD). From the above results, the performance of ACLD treatment with proportional controller is very effective as low frequencies. And the augmenting the control law with a derivative component is found to extend the effectiveness of the plate/ACLD system over wider frequency band.

Table 7 The natural frequencies, loss factors and attenuations of the first bending mode for full ACLD treatment at temperature 25℃

T:25°C	First bending mode			
k_p(only)	Frequency	Loss factor	Amplitude	Attenuation
k_p=00	4.48	0.042	236.14	
k_p=30	4.60	0.052	166.56	29.4%
k_p=60	4.75	0.073	113.12	52.3%
k_p=120	5.00	0.130	64.80	72.4%

Table 8 The natural frequencies, loss factors and attenuations of the second bending mode for full ACLD treatment at temperature 25℃

T:25°C	Second bending mode			
k_p(only)	Frequency	Loss factor	Amplitude	Attenuation
k_p=00	27.58	0.042	75.98	
k_p=30	28.06	0.041	76.00	-0.02%
k_p=60	28.15	0.039	77.88	-2.3%
k_p=120	28.37	0.036	84.36	-11.5%

Table 9 The natural frequencies, loss factors and attenuations of the first bending mode for full ACLD treatment at temperature 25℃

T:25°C	First bending mode			
k_p, k_d	Frequency	Loss factor	Amplitude	Attenuation
k_p=00, k_d=00	4.48	0.042	236.14	
k_p=30, k_d=50	4.65	0.075	131.18	44.4%
k_p=60, k_d=130	4.75	0.147	58.42	75.3%
k_p=120, k_d=220	4.94	0.182	43.82	81.4%

Table 10 The natural frequencies, loss factors and attenuations of the second bending mode for full ACLD treatment at temperature 25℃

T:25°C	Second bending mode			
k_p, k_d	Frequency	Loss factor	Amplitude	Attenuation
k_p=00, k_d=00	27.58	0.042	75.98	
k_p=30, k_d=50	27.80	0.046	66.97	11.9%
k_p=60, k_d=130	28.00	0.060	53.05	30.2%
k_p=120, k_d=220	27.96	0.133	32.11	57.7%

8. COMPARISON BETWEEN THEORETICAL AND EXPERIMENTAL RESULTS

The characteristic eigenvalue equations of the plate/ACLD are obtained from the following resulting equations:

$$\{[K]-\omega^{*2}[M]\}\{\Phi\}=0, \tag{73}$$

where $\omega*$ is the radian frequency (rad/sec) and $\{\Phi\}$ is the corresponding eigenvector. The eigenvalues in the equation (73) are solved using the IMSL complex value subroutine. This yields complex eigenvalues which are expressed as follows:

$$\omega^{*2}=\omega^2(1+i\eta), \tag{74}$$

where η is the loss factor of the plate/ACLD corresponding to the modal frequency ω. Moreover, the numerical integrations of the stiffness, mass and force matrices are performed using the Gaussian technique[6]. Hence, the theoretical results are directly compared with the experimental results.

The theoretical modal parameters, evaluated by the finite element method, are experimentally verified for the first two bending modes with different control gains at temperature 25℃. Tables 11 and 12 show such comparisons when the full ACLD treatment is controlled with a proportional controller and a derivative controller. The results show a good agreement between theory and experiment. The discrepancy is

about 35% in the modal frequencies and about 46% in the modal damping ratios respectively. It is evident that increasing the derivative control gains have a significant effect on improving the damping ratio characteristics of the second bending mode.

Figs. 8 through 9 summarize these results for different control gains for the full treatment plate/ACLD system. Close agreement between theoretical predictions and experimental measurements is evident.

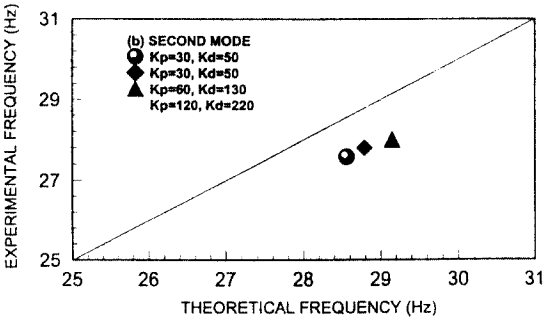

(a) first bending mode

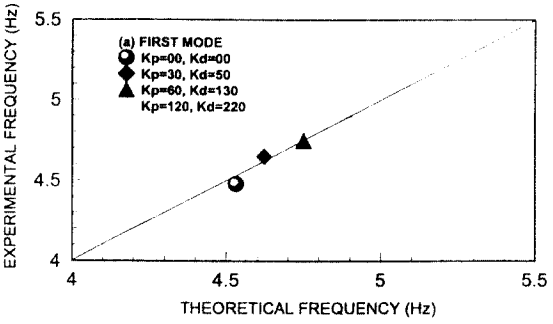

(b) second bending mode

Fig. 8 Comparison between theoretical and experimental natural frequencies controlled by various k_p and k_d

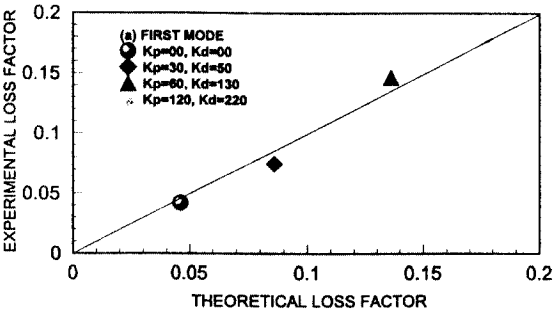

(a) first bending mode

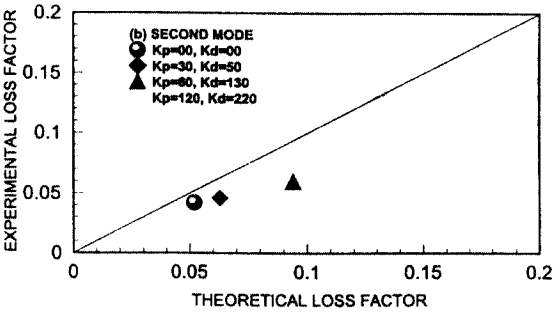

(b) second bending mode

Fig. 9 Comparison between theoretical and experimental loss factors controlled by various k_p and k_d

Table 11 The comparison between theoretical and experimental natural frequencies and loss factors of the 1st bending mode for full ACLD treatment at temperature 25℃

T:25°C (1st Mode)	Experimental Results		Theoretical Results	
k_p, k_d	Frequency	Loss factor	Frequency	Loss factor
k_p=00, k_d=00	4.48	0.042	4.53	0.046
k_p=30, k_d=50	4.65	0.075	4.62	0.086
k_p=60, k_d=130	4.75	0.147	4.75	0.136
k_p=120, k_d=220	4.94	0.182	4.88	0.177

Table 12 The comparison between theoretical and experimental natural frequencies and loss factors of the 2nd bending mode for full ACLD treatment at temperature 25℃

T:25°C (2nd Mode)	Experimental Results		Theoretical Results	
k_p, k_d	Frequency	Loss factor	Frequency	Loss factor
k_p=00, k_d=00	27.58	0.042	28.56	0.052
k_p=30, k_d=50	27.80	0.046	28.79	0.063
k_p=60, k_d=130	28.00	0.060	29.15	0.094
k_p=120, k_d=220	27.96	0.133	29.53	0.132

9. CONCLUSIONS

In this paper, a theory that was capable of incorporating the piezoelectric sensor/actuator equation and shear effects of viscoelastic equation into the governing equation of the plate/ACLD system was formulated using two methods. The first method was based on the Newton's law which described the dynamic behavior of plate/ACLD system under the action of the applied electric field. The second method was the Hamilton's principle which required the minimization of the total potential energy to derive the equations of motion and associated boundary. A comparison between the governing equations of motion using two methods has been verified that their results are identical. Also, the effectiveness of a new class of active constrained layer damping (ACLD) treatment for plates in vibration damping has been theoretically and experimentally verified. This effectiveness was achieved through the use of simple proportional controller with a derivative component to enhance its capabilities at high frequencies. Hence, the developed theoretical and experimental techniques present invaluable tools for designing and predicting the performance of the smart laminated structures that can be used in many engineering applications.

ACKNOWLEDGEMENT

The author would like to express his deep sense of gratitude to Professor Amr Baz for his continued guidance and invaluable discussions throughout this research. Also, the present work was carried out as a sabbatical year program of the second author by financial support from Gyeongsang National University.

REFERENCES

1) Ghoneim, H., "lectromechanical Surface Damping Using Constrained Layer and Shunted Piezoelectric", SPIE Proceedings: Smart Materials and Structures, Vol. 1919-8, pp. 78~89, 1993
2) Y. Shen, "Bending Vibration Control of Composite and Isotropic Plates through Intelligent Constrained Layer Treatments", J. of Smart Materials and Structures, Vol.3, pp. 59~70, 1994
3) Y.V.K.S. Rao and B. C. Nakra, "Vibrations of unsymmetrical sandwich beams and plates with viscoelastic cores", J. of Sound and Vibration, 34(3), 309~326, 1974
4) Alam, N. and Asnani, N. T., "Vibration

and damping analysis of multilayered rectangular plates with constrained viscoelastic layers", J. of Sound and Vibration, 97(4), pp. 597~614, 1984

5) C. K. Lee, "Piezoelectric Laminates for Torsional and Bending Modal Control: Theory and Experiment.", Ph.D thesis. Cornell University, Ithaca, NY. 1987

6) C. Zienkiewicz, "The Finite Element Method", McGraw-Hill, New York, 1977

7) C. H. Park and A. Baz, "Vibration Control of Bending Modes of Plates Using Active Constrained Layer Damping", Journal of Sound and Vibration, submitted 1996